HHS Public Access

Author manuscript

Cancer Res. Author manuscript; available in PMC 2021 July 10.

Published in final edited form as:

Cancer Res. 2018 November 01; 78(21): 6098–6106. doi:10.1158/0008-5472.CAN-17-3600.

Heterozygosity of Chaperone Grp78 Reduces Intestinal Stem Cell Regeneration Potential and Protects against Adenoma Formation

Jooske F. van Lidth de Jeude[1], **Claudia N. Spaan**[1], **Bartolomeus J. Meijer**[1], **Wouter L. Smit**[1], **Tanya T.D. Soeratram**[1], **Mattheus C.B. Wielenga**[1], **B. Florien Westendorp**[1], **Amy S. Lee**[2], **Sander Meisner**[1], **Jacqueline L.M. Vermeulen**[1], **Manon E. Wildenberg**[1], **Gijs R. van den Brink**[1], **Vanesa Muncan**[1], **Jarom Heijmans**[1,3]

[1]Department of Gastroenterology and Hepatology, Tytgat Institute for Liver and Intestinal Research, University of Amsterdam, Amsterdam, the Netherlands. [2]Department of Biochemistry and Molecular Medicine, USC/Norris Comprehensive Cancer Center, Keck School of Medicine, University of Southern California, Los Angeles, Los Angeles, California. [3]Department of Internal Medicine, University of Amsterdam, Amsterdam, the Netherlands.

Abstract

Deletion of endoplasmic reticulum resident chaperone Grp78 results in activation of the unfolded protein response and causes rapid depletion of the entire intestinal epithelium. Whether modest reduction of Grp78 may affect stem cell fate without compromising intestinal integrity remains unknown. Here, we employ a model of epithelial-specific, heterozygous *Grp78* deletion by use of *VillinCre*^{ERT2}-*Rosa26*$^{ZsGreen/LacZ}$-*Grp78*$^{+/fl}$ mice and organoids. We examine models of irradiation and tumorigenesis, both *in vitro* and *in vivo*. Although we observed no phenotypic changes in *Grp78* heterozygous mice, *Grp78* heterozygous organoid growth was markedly reduced. Irradiation of *Grp78* heterozygous mice resulted in less frequent regeneration of crypts compared with nonrecombined (wild-type) mice, exposing reduced capacity for self-renewal upon genotoxic insult. We crossed mice to *Apc*-mutant animals for adenoma studies and found that

Corresponding Author: Jarom Heijmans, University of Amsterdam, Meibergdreef 69–71, Amsterdam 1105 BK, the Netherlands. Phone: 312-0566-8873; Fax: 312-0566-9190; j.heijmans@amc.nl.

Current address for G.R. van den Brink: GlaxoSmithKline, Medicines Research Center, Stevenage, United Kingdom.

Authors' Contributions

Conception and design: J.F. van Lidth de Jeude, M.C.B. Wielenga, G.R. van den Brink, J. Heijmans

Development of methodology: J.F. van Lidth de Jeude, M.C.B. Wielenga, J. Heijmans

Acquisition of data (provided animals, acquired and managed patients, provided facilities, etc.): J.F. van Lidth de Jeude, C.N. Spaan, B.J. Meijer, W.L. Smit, M.C.B. Wielenga, B.F. Westendorp, A.S. Lee, S. Meisner, J. Heijmans

Analysis and interpretation of data (e.g., statistical analysis, biostatistics, computational analysis): J.F. van Lidth de Jeude, C.N. Spaan, B.J. Meijer, W.L. Smit, S. Meisner, G.R. van den Brink, J. Heijmans

Writing, review, and/or revision of the manuscript: J.F. van Lidth de Jeude, C.N. Spaan, B.J. Meijer, W.L. Smit, A.S. Lee, M.E. Wildenberg, G.R. van den Brink, V. Muncan, J. Heijmans

Administrative, technical, or material support (i.e., reporting or organizing data, constructing databases): J.F. van Lidth de Jeude, W.L. Smit, T.T.D. Soeratram, B.F. Westendorp, J.L.M. Vermeulen, J. Heijmans

Study supervision: M.E. Wildenberg, G.R. van den Brink, V. Muncan, J. Heijmans

Disclosure of Potential Conflicts of Interest

No potential conflicts of interest were disclosed.

Note: Supplementary data for this article are available at Cancer Research Online (http://cancerres.aacrjournals.org/).

adenomagenesis in *Apc* heterozygous-*Grp78* heterozygous mice was reduced compared with *Apc* heterozygous controls (1.43 vs. 3.33; $P < 0.01$). In conclusion, epithelium-specific *Grp78* heterozygosity compromises epithelial fitness under conditions requiring expansive growth such as adenomagenesis or regeneration after γ-irradiation. These results suggest that Grp78 may be a therapeutic target in prevention of intestinal neoplasms without affecting normal tissue.

Introduction

The intestinal epithelium undergoes continuous renewal with the lifespan of intestinal epithelial cells being 4 to 5 days (1). The massive amount of cells required to maintain this process is derived from a pool of stem cells that reside at the bottom of intestinal crypts (2). In addition to their role to maintain the epithelium during homeostasis, stem cells play a key role in processes like tissue wound repair and they are regarded as the cell of origin of intestinal cancer (3). The balance between stem cell proliferation and differentiation must therefore be stringently controlled. Damaged stem cells that may have impaired functioning must thus be weeded out to maintain a healthy stem cell pool. Processes that detect damage in intestinal epithelial stem cells and deplete such cells by apoptosis or forced differentiation are therefore critical for maintenance of integrity of the organism, but these processes have not been fully characterized.

We have previously identified the unfolded protein response (UPR) as a pathway that can cause rapid loss of intestinal epithelial stem cells (4). This pathway senses accumulation of unfolded and malfolded proteins inside the endoplasmic reticulum (ER) that may result from various stimuli in homeostatic or pathophysiologic conditions, including differentiation, hypoxia, inflammation, and γ-irradiation (5–8). Unfolded proteins accumulate inside the ER, which is sensed as ER stress and attract chaperones to reduce aggregation of proteins and facilitate processing and folding (9). The 78-kDa glucose regulated protein (GRP78), also referred to as BiP/HSPA5, is a critical ER luminal chaperone with potent antiapoptotic properties playing critical roles in development and human diseases (10, 11). In addition to its role as a chaperone, GRP78 is a key regulator of the UPR. Under homeostatic conditions, it binds the three ER transmembrane sensors IRE1α, ATF6, and PERK and maintains them in their inactive state (12). Upon accumulation of malfolded proteins in the ER, GRP78 is dissociated from these transmembrane sensors and UPR signaling is initiated. Signaling of IRE1α and ATF6 results in upregulation of ER components and increased ER capacity. Kinase PERK phosphorylates translation initiation factor eIF2α, which results in temporary attenuation of global protein translation. These three branches of UPR signaling seek to restore homeostasis in the ER in an orchestrated fashion. If homeostasis is not achieved, persistent activation of the UPR, through upregulation of proapoptotic factors such as CHOP results in apoptosis.

Stress in the ER (ER stress) activates the UPR, which results in rapid loss of homeostatic intestinal epithelial stem cells as well as malignantly transformed stem cells that have obtained homozygous oncogenic mutations in the *APC* gene (4, 13). Moreover, induction of ER stress in cells derived from human colorectal cancer resulted in increased chemosensitivity and differentiation (14).

In previous studies, we have induced ER stress by genetic knockout of both *Grp78* alleles from the intestinal epithelium. In contrast to the phenotype of *Grp78* knockout, body-wide heterozygous expression of *Grp78* in mice did not result in altered bodyweight or altered organ histology compared with wild-type littermate controls (15, 16). In addition, heterozygous *Grp78* expression was sufficient for normal production of immunoglobulins in plasma cells that are known to exhibit one of the highest levels of protein production (16, 17). Upon induction of pancreatitis, however, $Grp78^{+/-}$ mice did exhibit increased severity of pancreatitis, with increased expression of proapoptotic gene Chop (18). In a similar fashion, *Chop* expression was increased in mammary tumors of $Grp78^{+/-}$ mice compared with tumors in *Grp78* wild-type mice (16).

Thus, although heterozygous expression of *Grp78* does not result in a detectable phenotype under homeostatic conditions, the reduced capacity of the ER may result in enhanced ER stress sensing and a lower threshold of UPR activation during situations that require ER capacity and induce accumulation of malfolded proteins.

Damaged cells should be removed by quality control mechanisms and UPR signaling may play such a role in the intestinal epithelium. We hypothesize that increasing the sensitivity of the ER to stimuli that depend on ER capacity protects the intestinal stem cell during situations of intestinal damage and tumorigenesis.

Materials and Methods

Animal experiments

All mouse experiments were performed in the Academic Medical Center Animal Research Institute in accordance with local guidelines and all experiments were reviewed and approved by the local review board. $VillinCre^{ERT2}$, $Rosa26^{LacZ}$, Apc^{fl}, and $Grp78^{fl}$ alleles were all described previously (19–24). $Apc^{min/+}$ mice (25) were obtained from The Jackson Laboratory.

For Cre^{ERT2}-mediated recombination, mice were given five injections of 50 mg/kg tamoxifen (Sigma-Aldrich, 10 mg/mL in corn oil), on 5 consecutive days. Two hours prior to sacrifice, all mice received 100 mg/kg BrdU intraperitoneally (Sigma-Aldrich, 10 mg/mL in PBS). After sacrifice, intestines were immediately taken out and rinsed in cold PBS.

Mice were irradiated with 14 Gy γ-irradiation, 2 weeks after the last injection with tamoxifen.

Adenomas were counted blinded by 3 different people, both macroscopically and microscopically, including adenomas of 1 mm or larger.

Males and females were distributed equally among each genotype. In general and irradiation experiment, mice were sacrificed at approximately 10 weeks of age. In the adenoma experiment, mice were sacrificed at 20 weeks of age. For all experiments, littermate controls were used.

Tissue preparation, IHC, and X-Gal staining

Tissue was fixed in 4% buffered formaldehyde in PBS. The next day, formalin was replaced with 70% ethanol and processed according to standard protocols for paraffin embedding. After paraffin embedding, 4-μm sections were made and used for routine hematoxylin and eosin staining. IHC was performed as described previously (26). In short, 4-μm sections were deparaffinized and rehydrated. Endogenous peroxidase was blocked in 0.3% H_2O_2 in methanol. For antigen retrieval, slides were treated at 96°C for 10 minutes in 10 mmol/L sodium citrate buffer pH 6.0, or for 20 minutes in 10 mmol/L Tris 1 mmol/L EDTA buffer pH 9.0 and incubated overnight at 4°C with primary antibody diluted in PBT (PBS with 0.1% Triton X-100 and 1% w/v BSA). The following primary antibodies were used: anti-BrdU mouse monoclonal 1:500 (Roche, BMC9318) and anti-cleaved-caspase-3 (Cell Signaling Technology, 9661S). Antibody binding was visualized with Powervision (Immunologic) and substrate development was performed using diaminobenzidine (Sigma-Aldrich, D5637–10G). Hematoxylin was used as counterstain.

For assessment of recombination efficacy, cells expressing the LacZ allele were visualized with X-Gal staining. This was performed by fixing freshly isolated tissues for 90 minutes at 4°C in PBS containing 1% formaldehyde, 0.2% glutaraldehyde, and 0.02% NP-40. Tissue was washed in ice-cold PBS subsequently and stained overnight in a dark chamber using PBS containing 5 mmol/L K3Fe(CN)6, 5 mmol/L K4Fe(CN)6, 2 mmol/L MgCl2, 1 mg/mL X-Gal, and 0.02% NP-40. After X-Gal staining, tissue was postfixed in 4% buffered formaldehyde in PBS and processed as described previously. Counterstaining of sections was performed with nuclear fast red. Quantification of stainings was done in 30 crypts per animal in a blinded manner.

ISH

For conventional ISH, we used methods described previously (13), using *mRNA* antisense probes (sequence available upon request). RNAscope experiments were performed using RNAscope, an RNA ISH technique described previously (27). RNAscope was performed according to the “Formalin-Fixed Paraffin-Embedded Sample Preparation and Pretreatment for RNAscope 2.5 assay” and “RNAscope 2.5 HD Detection Reagent – RED” protocols as provided by the manufacturer.

For RNAscope, the following probes were used: mm_Olfm4 (REF 311831, LOT16224A).

For *in situ* assessment of the $Grp78^{\Delta 5-7}$ *mRNA*, The BaseScope Reagent Kit (Advanced Cell Diagnostics) was used according to the manufacturer’s instructions using a custom designed mmHspa5 probe targeting nucleotides 613–1399 of the *mRNA*.

Organoid culture

Organoids from primary intestinal epithelium were obtained from mice with indicated genotypes. Harvest and expansion of intestinal organoid culture was performed as described previously (4, 28, 29). Recombination of organoids was established by adding 1 μmol/L 4OHT (Sigma-Aldrich, H6278–10MG) to culture medium for 24 hours at 48 hours after passaging unless stated otherwise. 4OHT in ethanol was added to culture medium

(1:1,000).Ethanol was used as vehicle. In irradiation experiments, organoids were subjected to 6 Gy γ-irradiation, 24 hours after recombination. Where indicated, we cultured organoids with 5 μmol/L CHIR-99021 (Sellekchem, S126307).

Measuring global translation rates

To measure global protein synthesis rates, we quantified the incorporation of ^{35}S-labeled methionine and cysteine into newly translated proteins. Organoids were grown for 4 days after passaging in 48-well plates (20 μL of Matrigel per well). Recombination was induced from 48 hours, and growth factors (EGF, R-spondin, Noggin) were withdrawn 24 hours prior to the incorporation assay. Organoids were exposed to a 15-minute methionine starvation followed by a 45-minute pulse with 1 μL (1,25 μCi/mL) of EasyTag L-[35S]-Methionine, (PerkinElmer) per well. After labeling, organoids were washed twice in ice-cold PBS, harvested, and centrifuged in cold PBS to remove supernatant and Matrigel fragments. Next, cell pellets were lysed in cell lysis buffer (Cell Signaling Technology). Fifteen microliters of radioactive lysate was blotted on labeled 24-mm glass microfiber filters (GF/C Whatman) that were presoaked in 20% tri-chloro-acetic acid (TCA). Filters were dried and placed in a vacuum manifold and incubated in 10% ice-cold TCA for 15 minutes, followed by 10% TCA at 90°C to 95°C for 10 minutes to break any aminoacyl-tRNA bonds. Filters were washed twice with cold 2% TCA and then twice with 95% ethanol to remove TCA. Dried filters (> 1 hour) were placed in liquid scintillation cocktail (Ultima Gold, PerkinElmer) for 2 hours and radioactive decay was quantified using a scintillation counter (Tri-Carb 2900TR). Counts per minute were calculated relative to control samples and presented as percentage of control.

Separation of intestinal epithelial cell fractions

Tissue was harvested in PBS, and 2-cm pieces of whole intestine were used for further processing to obtain pure epithelial fractions that did not contain mesenchyme (30). In short, the pieces of intestine were incubated for exactly 7 minutes in 30 mmol/L EDTA in HBSS at 37°C. After incubation, samples were vortexed and centrifuged, after which, the supernatant containing the epithelial fraction was decantated and centrifuged again.

RNA isolation

For gene expression experiments in organoids, *mRNA* isolation was performed 24 hours after treatment with 4OHT using the Bioline ISOLATE II RNA Mini Kit (BIO-52073, Bioline) according to the manufacturer's instructions. For RNA extraction from mouse intestine, tissue was homogenized with a Miccra D-1 homogenizer in 1 mL Tri-reagent (T9424, Sigma-Aldrich) and RNA extraction was performed according to the manufacturer's protocol.

cDNA synthesis and qRT-PCR

Synthesis of cDNA was performed using 1 μg of purified RNA using Revertaid reverse transcriptase according to protocol (Fermentas). qRT-PCR was performed using sensifast SYBR No-ROX Kit (GC-biotech, Bio-98020) according to the manufacturer's protocol on a BioRad iCycler. Primers sequences were ordered as found on qPrimerdepot

(mouseprimerdepot.nci.nih.gov/). All primer sets were intron spanning. Primer specificity was tested using melting curve analysis. Relative gene expression was calculated using the $2^{-\Delta Ct}$ method, with *actin* as reference gene.

Immunoblotting

Cells were lysed in cell lysis buffer (Cell Signaling Technology), and boiled in sample buffer containing 0.25 mol/L Tris-HCl pH 6.8, 8% SDS, 30% glycerol, 0.02% bromophenol blue, and 1% β-mercaptoethanol. Separation was done on 10% SDS-PAGE, and proteins were transferred to a polyvinylidene difluoride membrane. Specific detection was done by incubating the blot overnight in TBS with 0.1% Tween-20 with 1% BSA. Antibody binding was visualized using the Lumi-Light Western Blotting Substrate (Roche). The following antibodies were used: actin (Sigma, Ab1978), Grp78 (Cell Signaling Technology, 3177S), and c-Myc (Santa Cruz Biotechnology, sc-764). Quantifications of blots were performed with ImageJ software.

Statistical analysis

Statistical analysis was performed using GraphPad Prism 5.0 software. All values are depicted as the mean ± SEM. In experiments comparing two groups, statistical significance was analyzed using Student *t* test. For multiple comparisons, one-way or two-way ANOVA was used followed by a Bonferroni *post* test. All organoid experiments were done in triplicate, with 3 wells of organoids per condition. In all mouse experiment, $n = 10$ for each genotype. In each mouse experiment, we assumed effects to be 50% compared with controls, on the basis of the previous experiments performed in our laboratory. To predict effects in the $Apc^{het(IEC)}$ model, we performed power calculations based on previous experiments in $Apc^{min/+}$ mice, each developing 100 ± 39 polyps/animal.

Differences were considered statistically significant at $P < 0.05$.

Results

Reduced levels of Grp78 in intestinal organoids result in reduced stemness and proliferation, with increased sensitivity to irradiation and increased growth factor dependency

To assess the effects of reduced levels of *Grp78*, we generated mice that were heterozygous for a conditional allele that allows deletion of *Grp78*. These mice were crossed to $Villin^{CreERT2}$ mice for intestinal epithelium–specific tamoxifen-inducible deletion of a single allele of *Grp78*. In addition, mice were crossed to $Rosa26^{ZsGreen}$ reporter mice or $Rosa26^{LacZ}$ reporter mice to enable visualization of recombination efficacy after Cre-mediated recombination. From these $Villin^{CreERT2}$-$Rosa26^{ZsGreen/LacZ}$-$Grp78^{+/fl}$ mice, we generated intestinal epithelial $Villin^{CreERT2}$-$Rosa26^{ZsGreen/LacZ}$-$Grp78^{+/fl}$ organoids (next referred to as $Grp78^{+/fl}$), in which *Cre*-mediated deletion of a single *Grp78* allele could be established by addition of tamoxifen metabolite 4OHT to the culture medium, resulting in $Villin^{CreERT2}$-$Rosa26^{ZsGreen/LacZ}$-$Grp78^{+/-}$ organoids (next referred to as $Grp78^{+/-}$). Recombination efficacy was monitored using the fluorescent *ZsGreen* allele.

After 48 hours of treatment with 4OHT, all *Grp78*$^{+/-}$ organoids were green fluorescent (Fig. 1A). In the *Grp78* conditional allele, exons 5 to 7 are removed by *Cre*-mediated recombination. Although nonfunctional, expression of the remaining floxed *Grp78*$^{\Delta 5-7}$ *mRNA* can still be measured, as has been described previously (24). Using a specific primer set that spans exons 5 to 7, we assessed expression of the *Grp78*$^{\Delta 5-7}$ *mRNA* and found high expression, whereas this was not discernible in wild-type or nonrecombined *Grp78*$^{+/fl}$ organoids (Fig. 1B). Performing Western blot analysis, we found reduced Grp78 protein levels in *Grp78*$^{+/-}$ organoids (Fig. 1C and D). We next assessed proliferative potential of *Grp78*$^{+/-}$ organoids and found that organoids that lacked a single *Grp78* allele had reduced growth potential (Fig. 1E). Growth retardation was accompanied by increased expression of several markers of UPR activation 3 days after recombination, in particular *Chop*, a target of the PERK-eIF2α UPR signaling pathway (Fig. 1F). In addition, we observed reduced levels of crypt base columnar cell (CBC) stem cell markers *Lgr5* and *Olfm4* in *Grp78*$^{+/-}$ organoids.

To assess whether heterozygous expression of *Grp78* increased sensitivity of these organoids to circumstances that cause reduced growth, we cultured organoids in medium containing reduced levels of the critical growth factor Rspondin1 (Rspo1). Reduced levels of Rspo1 in the culture medium slightly reduced growth of wild-type organoids (Supplementary Fig. S1A). In *Grp78*$^{+/-}$ organoids, however, Rspo1 reduction caused significant growth impairment (Supplementary Fig. S1B). In addition, a similar effect was seen upon γ-irradiation of organoids. Irradiated wild-type organoids showed reduced budding after two days compared with nonirradiated organoids with a rapid recovery at day 4 (91.7% vs. 98.3%, ns). In *Grp78*$^{+/-}$ organoids, growth was reduced in nonirradiated organoids compared with wild-type organoids (49.3% vs. 98.3%; $P < 0.001$) and further impaired by irradiation (17.8% vs. 49.3%; $P < 0.001$; Supplementary Fig. S1C).

Organoids are cultured in standard culture conditions, with approximately 21% oxygen. Because oxygen tension in the intestinal mucosa is low (31), we examined whether reduced growth of *Grp78*$^{+/-}$ organoids resulted from reduced capacity to cope with a high oxygen tension environment containing increased reactive oxygen species (ROS). To this end, we examined expression of CBC markers *Lgr5, Olfm4* under circumstances of low oxygen (5% O_2). We found no different expression of these markers in both nonrecombined and *Grp78*$^{+/-}$ organoids when compared with 20% O_2 (Supplementary Fig. S1D).

Heterozygosity of *Grp78* in organoids thus increased expression of markers of activation of the UPR and resulted in reduced growth potential, most strikingly during circumstances of reduced availability of growth factors or damage by irradiation.

Grp78 heterozygosity has no discernible effect on intestinal homeostasis

Organoids of intestinal epithelium are continuously expanding cell cultures. Expansion of these structures is driven by crypt fissioning and crypt budding, which are processes that are characteristic of intestinal growth and repair. Organoids do, therefore, not completely mimic homeostatic intestinal epithelium, where crypt numbers are maintained stable. Effects of *Grp78* heterozygosity observed *in vitro* in organoids may therefore be distinct from the effects in the homeostatic intestinal epithelium in unchallenged mice *in vivo*. We next

examined inducible *Villin*^{CreERT2}-*Rosa26*$^{ZsGreen/LacZ}$-*Grp78*$^{+/fl}$ mice, in which *Grp78* heterozygosity in intestinal epithelial cells (IEC) could be established after injections with tamoxifen, resulting in *Villin*^{CreERT2}-*Rosa26*$^{ZsGreen/LacZ}$-*Grp78*$^{+/-}$ mice (next referred to as *Grp78*$^{het(IEC)}$). To control for off-target effects of tamoxifen, we used littermate *Villin*^{CreERT2}- *Rosa26*$^{ZsGreen/LacZ}$-*Grp78*$^{+/+}$ mice that had received injections with tamoxifen as controls (next referred to as *Grp78*^{wt}).

Expression of the *LacZ* reporter allele showed that one month after recombination, nearly 100% of crypts remained recombined in *Grp78*$^{het(IEC)}$ and *Grp78*^{wt} control animals (Fig. 2A) and similar to recombined organoids, expression of the floxed *Grp78*$^{\Delta 5-7}$ *mRNA* was high in *Grp78*$^{het(IEC)}$ animals as shown by qRT-PCR (Fig. 2B). To confirm recombination throughout the intestinal epithelium of *Grp78*$^{het(IEC)}$ animals, we generated an RNA probe that spanned the junction between exons 4 and 8 and was thus capable of detecting the floxed *Grp78*$^{\Delta 5-7}$ *mRNA* specifically. We used single-molecule *mRNA* labeling *ISH* to identify cells that expressed the floxed *Grp78*$^{\Delta 5-7}$ *mRNA* and found ubiquitous expression throughout the intestinal epithelium, confirming the extent of recombination (Supplementary Fig. S2). In addition, Grp78 protein levels were reduced in *Grp78*$^{het(IEC)}$ mice (Fig. 2C and D). *Grp78*$^{het(IEC)}$ animals had an unaltered rate of epithelial proliferation as judged by a 2-hour pulse of BrdU incorporation (Fig. 2E) Numbers of stem cells were unaltered in *Grp78*$^{het(IEC)}$ animals, as judged by quantification of cells that were labeled by ISH for CBC stem cell marker *Olfm4* (Fig. 2F and G). Quantification of markers of activation of the UPR showed mild increased expression of *p58*^{ipk}, whereas other markers were unaltered (Fig. 2H). We assessed *mRNA* expression levels of stem cell markers *Lgr5* and *Olfm4*, and found reduced *mRNA* levels, although stem cell numbers or proliferation, were thus not reduced. In addition, we assessed *mRNA* levels of alternative stem cell markers *Bmi1* and *HopX* that label + 4 cells and found these markers to be unaffected. Interestingly, we found a significant increase in expression of quiescent stem cell marker *mTert* (Supplementary Fig. S3; refs 32–34).

Considering the differences between expanding growth in organoids and homeostatic growth in mice, we conclude that *Grp78* heterozygosity results in growth reduction in situations of exaggerated or expanded growth, but not during homeostatic proliferation.

Grp78 heterozygosity results in reduced self-renewal capacity during tissue regeneration

During insults that damage the intestine, expansive growth is required for tissue repair and cells with reduced growth capacity have impaired regenerative capacity. Moreover, the regenerative response shares features with organoid growth, such as fissioning and budding of crypts.

We subjected *Grp78*$^{het(IEC)}$ animals and *Grp78*^{wt} controls to 14 Gy γ-irradiation. After 48 hours, we observed epithelial damage, such as aberrant stacking of enterocytes and presence of apoptotic bodies (Supplementary Fig. S4A). After 96 hours, a regenerative response was observed in all intestines regardless of genotype (Supplementary Fig. S4B).

All mice carried a LacZ reporter allele to assess recombination efficacy. Near-complete recombination was observed for both wild-type and heterozygous animals at 48 hours after

irradiation (91% vs. 82%, $P = 0.258$, Fig. 3A and B). Strikingly, at 96 hours after recombination, a significant increase in the amount of nonrecombined (wild-type) crypts could be observed in *Grp78*$^{het(IEC)}$ animals, but not in controls (49% vs. 51%, $P < 0.05$, Fig. 3A and B).

We tested *mRNA* expression levels of the *LacZ* gene-product and confirmed reduced *LacZ* expression and thus loss of the recombined *Grp78* allele in *Grp78*$^{het(IEC)}$ cells at the mRNA level (Fig. 3C). To assess whether these differences could be the effect of increased apoptosis in *Grp78*$^{het(IEC)}$ animals, we quantified cleaved caspase-3^{+} apoptotic cells and found no significant differences compared with controls (Fig. 3D and E). These results show that in *Grp78*$^{het(IEC)}$ intestines, regeneration is favored from nonrecombined stem cells rather than from stem cells that have reduced levels of *Grp78*.

Grp78 heterozygosity protects from intestinal adenoma formation

Colorectal cancers develop from adenomas. The classical adenoma-initiating event is loss of the adenomatous polyposis coli (*APC*) tumor suppressor gene, which results in activation of the Wnt signaling pathway, leading to accumulation of stem cells, increased proliferation, crypt expansion, and crypt fissioning (24). Humans and mice that lack a single *APC* allele are prone for development of intestinal adenomas and in 80% of sporadic colorectal carcinomas a biallelic loss of *APC* is observed (35, 36).

To investigate adenoma development in *Grp78*$^{het(IEC)}$ mice, we generated mice with heterozygous deletion of both *Grp78* and *Apc* from the intestinal epithelium (*Apc-Grp78*$^{het(IEC)}$). Recombination of both single alleles was induced at the age of 4 weeks and mice were sacrificed for adenoma analysis at 20 weeks of age. We compared proliferation and adenoma formation in *Apc-Grp78*$^{het(IEC)}$ mice to *Apc*$^{het(IEC)}$ controls. As expected, *Apc*$^{het(IEC)}$ mice had increased epithelial proliferation compared with wild-type control animals, confirming efficacy of recombination (Fig. 4A). In recombined tissue, proliferation showed no significant difference between *Apc-Grp78*$^{het(IEC)}$ and *Apc*$^{het(IEC)}$ control epithelium. However, the average number of adenomas was significantly reduced in *Apc-Grp78*$^{het(IEC)}$ mice (Fig. 4B). We did however not observe differences in adenoma size between the two genotypes (Fig. 4C and D).

Because adenoma development is inhibitedin *Apc-Grp78*$^{het(IEC)}$ animals, reduced capacity of the ER because of Grp78 heterozygosity likely results in differentiation of cells that harbor increased ER-stress. To analyze whether adenoma development is accompanied by increased ER-stress and activation of the UPR, we performed *ISH* for a number of components of the UPR (*Erdj4*, *Chop*, and *Atf4*) on adenomatous and adjacent normal tissue of *Apc*$^{min/+}$ mice. We indeed observed increased expression of these UPR target *mRNAs* in adenomatous tissue, confirming increased activity of the UPR inside adenomas (Supplementary Fig. S5).

Thus, our results show that *Grp78* heterozygosity protects from intestinal adenoma formation, without causing growth defects on homeostatic tissue, potentially due to increased dependency on the capacity of the ER during adenomagenesis.

Because loss of *Apc*, through activation of the Wnt signaling pathway, has been found to increase global protein translation (37), we examined additional effects of *Grp78* heterozygosity. To this end, we treated *Grp78*$^{+/-}$ organoids with CHIR-99021, a GSK3β-inhibitor that results in activation of the Wnt pathway, resembling loss of *Apc* (38). Protein synthesis levels were reduced in *Grp78*$^{+/-}$ organoids, and although activation of the Wnt pathway by treatment with CHIR-99021 increased protein synthesis levels in controls, it failed to do so in *Grp78*$^{+/-}$ organoids (Fig. 5A).

Proliferation that results from hyperactivation of the Wnt signaling pathway is transduced by the oncogene c-Myc (39). Moreover, c-Myc is implemented in promoting translation (40). We examined effects of Grp78 heterozygosity on c-Myc expression in the presence of CHIR-99021 and found reduced levels of c-Myc in CHIR-99021–treated organoids upon deletion of a single Grp78 allele (Fig. 5B and C). Moreover, we found that Grp78 heterozygosity increased expression of several markers of ER stress during treatment with CHIR-99021 (Fig. 5D).

Thus, we find that in the context of hyperactivated Wnt signaling, translation and expression of oncogene c-Myc are markedly inhibited by *Grp78* heterozygosity, which may mechanistically explain reduced adenomagenesis in *Grp78*$^{het(IEC)}$ animals.

Discussion

Pathways that control the fitness of intestinal epithelial cells, in particular progenitor cells, maintain a healthy stem cell pool that is capable of maintaining the intestinal epithelium during damage and repair and is protected from tumorigenesis. One such pathway is the UPR, which detects stress inside the ER and causes loss of self-renewal capacity in stem cells in which ER-stress is detected (4, 41, 42).

Homozygous genetic ablation of UPR gatekeeper chaperone *Grp78* results in rapid loss of stem cells from the intestinal epithelium through activation of the UPR. In addition, deletion of *Grp78* results in loss of progenitor cells from the esophageal epithelium as well as from the inner cell mass from blastocysts (4, 24, 41). We generated mice in which *Grp78* is heterozygously deleted from the intestinal epithelium, which show no alterations under homeostatic conditions, confirming earlier reports that showed unaltered organ histology and function in body wide *Grp78*$^{+/-}$ mice under normal circumstances (16, 18). Interestingly, we do find slight alterations at the molecular level (downregulation of stem cell marker *Lgr5* and *Olfm4 mRNA*), although this did not result in reduced stem cell numbers or reduced epithelial proliferation.

In a number of nonhomeostatic conditions in organoids, such as increased expansion, reduction of growth factor Rspondin1, or γ-irradiation, we observed impaired proliferation showing that these conditions provoke haploinsufficiency. The fact that intestines of mice that have impaired expression of *Grp78* remain unaffected during homeostasis exposes a critical difference between ever-expanding organoid cultures and homeostatic growth in intestines that maintains a constant number of crypts.

In addition, we find that that *Grp78*$^{het(IEC)}$ epithelium in mice has reduced self-renewal capacity upon γ-irradiation, in which regeneration is favored from wild-type nonrecombined stem cells over stem cells that lack a single *Grp78* allele. Moreover, crossing *Grp78*$^{het(IEC)}$ mice to animals with a conditional *Apc* allele results in reduced adenoma numbers pointing toward reduction in tumor initiation. Both regeneration and tumor initiation are features that are contributed to stem cell function (3, 43), thereby showing that under these circumstances, *Grp78* stem cells exhibit haploinsufficiency. These results may be explained by the fact that protein synthesis capacity and expression of oncogene c-Myc are reduced by *Grp78* heterozygosity in the context of hyperactive Wnt signaling.

It has been demonstrated previously that *Grp78* exhibits haploinsufficiency—in several models including pancreatitis and mammary tumor formation, thereby showing that threshold levels of *Grp78* that suffice under homeostatic conditions may fail under pathologic conditions (16, 18, 44). Interestingly, in these reports, body-wide *Grp78*$^{+/-}$ mice were used, in which *Grp78*$^{+/-}$ immune cells, stromal cells, or vascular cells may have contributed to increased pancreatitis or reduced tumorigenesis. Subsequent analysis on conditional heterozygous knockout of *Grp78* in endothelial cells showed minimal effect on normal tissue microvessel density while causing severe reduction in tumor angiogenesis and metastatic growth (45). Furthermore, targeted heterozygous knockout of *Grp78* in bone marrow suppressed blast numbers without affecting normal hematopoiesis (46). Recently, using the *Pdx1*^{Cre}-*Ras*$^{G12D/+}$-*P53*$^{fl/+}$ model for pancreatic ductal carcinoma, it was shown that epithelium-specific heterozygosity of *Grp78* resulted in reduced tumorigenesis and increased survival of mice (47). Pancreatic ductal cells are known for their large translational capacity and dependence on the ER and thus on *Grp78* levels. Interestingly, we show that in intestinal epithelial cells, that are not regarded as cells with high levels of translational- or ER capacity, *Grp78* heterozygosity results in a similar protection from tumorigenesis.

Together, our studies establish a role for *Grp78* in tissue regeneration and adenoma formation, thereby putting forth Grp78 as a promising preventive target in the development of therapies for colorectal cancer (11).

Supplementary Material

Refer to Web version on PubMed Central for supplementary material.

Acknowledgments

This work was supported by grants from the Dutch Cancer Society (KWF/UVA 2013-6135 and KWF/Alpe 11053/2017-1) and by a grant from the Netherlands Organisation for Scientific Research (NOW-Veni 91615032).

References

1. Clevers H. The intestinal crypt, a prototype stem cell compartment. Cell 2013;154:274–84. [PubMed: 23870119]
2. Barker N, van Es JH, Kuipers J, Kujala P, van den Born M, Cozijnsen M, et al. Identification of stem cells in small intestine and colon by marker gene Lgr5. Nature 2007;449:1003–7. [PubMed: 17934449]

3. Barker N, Ridgway RA, van Es JH, van de Wetering M, Begthel H, van den Born M, et al. Crypt stem cells as the cells-of-origin of intestinal cancer. Nature 2009;457:608–11. [PubMed: 19092804]
4. Heijmans J, van Lidth de Jeude JF, Koo B-K, Rosekrans SL, Wielenga MCB, van de Wetering M, et al. ER stress causes rapid loss of intestinal epithelial stemness through activation of the unfolded protein response. Cell Rep 2013;3:1128–39. [PubMed: 23545496]
5. Iwakoshi NN, Lee AH, Glimcher LH. The X-box binding protein-1 transcription factor is required for plasma cell differentiation and the unfolded protein response. Immunol Rev 2003;194:29–38. [PubMed: 12846805]
6. Wouters BG, Koritzinsky M. Hypoxia signalling through mTOR and the unfolded protein response in cancer. Nat Rev Cancer 2008;8: 851–64. [PubMed: 18846101]
7. Kaser A, Lee A-H, Franke A, Glickman JN, Zeissig S, Tilg H, et al. XBP1 links ER stress to intestinal inflammation and confers genetic risk for human inflammatory bowel disease. Cell 2008;134:743–56. [PubMed: 18775308]
8. Nagelkerke A, Bussink J, van der Kogel AJ, Sweep FC, Span PN. The PERK/ATF4/LAMP3-arm of the unfolded protein response affects radioresistance by interfering with the DNA damage response. Radiother Oncol 2013; 108:415–21. [PubMed: 23891100]
9. Ron D, Harding HP. Protein-folding homeostasis in the endoplasmic reticulum and nutritional regulation. Cold Spring Harb Perspect Biol 2012;4 pii:a013177.
10. Ni M, Lee AS. ER chaperones in mammalian development and human diseases. FEBS Lett 2007;581:3641–51. [PubMed: 17481612]
11. Lee AS. Glucose-regulated proteins in cancer: molecular mechanisms and therapeutic potential. Nat Rev Cancer 2014;14:263–76. [PubMed: 24658275]
12. Bertolotti A, Zhang Y, Hendershot LM, Harding HP, Ron D. Dynamic interaction of BiP and ER stress transducers in the unfolded-protein response. Nat Cell Biol 2000;2:326–32. [PubMed: 10854322]
13. van Lidth de Jeude JF, Meijer BJ, Wielenga MC, Spaan CN, Baan B, Rosekrans SL, et al. Induction of endoplasmic reticulum stress by deletion of Grp78 depletes Apc mutant intestinal epithelial stem cells. Oncogene 2017;36:3397–405. [PubMed: 27819675]
14. Wielenga MC, Colak S, Heijmans J, van Lidth de Jeude JF, Rodermond HM, Paton JC, et al. ER-stress-induced differentiation sensitizes colon cancer stem cells to chemotherapy. Cell Rep 2015;13:490–4.
15. Ye R, Jung DY, Jun JY, Li J, Luo S, Ko HJ, et al. Grp78 heterozygosity promotes adaptive unfolded protein response and attenuates diet-induced obesity and insulin resistance. Diabetes 2010;59:6–16. [PubMed: 19808896]
16. Dong D, Ni M, Li J, Xiong S, Ye W, Virrey JJ, et al. Critical role of the stress chaperone GRP78/BiP in tumor proliferation, survival, and tumor angiogenesis in transgene-induced mammary tumor development. Cancer Res 2008;68:498–505. [PubMed: 18199545]
17. Lee YK, Brewer JW, Hellman R, Hendershot LM. BiP and immunoglobulin light chain cooperate to control the folding of heavy chain and ensure the fidelity of immunoglobulin assembly. Mol Biol Cell 1999; 10:2209–19. [PubMed: 10397760]
18. Ye R, Mareninova OA, Barron E, Wang M, Hinton DR, Pandol SJ, et al. Grp78 heterozygosity regulates chaperone balance in exocrine pancreas with differential response to cerulein-induced acute pancreatitis. Am J Pathol 2010;177:2827–36. [PubMed: 20971738]
19. el Marjou F, Janssen K-P, Chang BH-J, Li M, Hindie V, Chan L, et al. Tissue-specific and inducible Cre-mediated recombination in the gut epithelium. Genesis 2004;39:186–93. [PubMed: 15282745]
20. Soriano P. Generalized lacZ expression with the ROSA26 Cre reporter strain. Nat Genet 1999;21:70–1. [PubMed: 9916792]
21. Madisen L, Zwingman TA, Sunkin SM, Oh SW, Zariwala HA, Gu H, et al. A robust and high-throughput Cre reporting and characterization system for the whole mouse brain. Nat Neurosci 2010;13:133–40. [PubMed: 20023653]
22. Shibata H, Toyama K, Shioya H, Ito M, Hirota M, Hasegawa S, et al. Rapid colorectal adenoma formation initiated by conditional targeting of the Apc gene. Science 1997;278:120–3. [PubMed: 9311916]

23. Sansom OJ, Reed KR, Hayes AJ, Ireland H, Brinkmann H, Newton IP, et al. Loss of Apc invivo immediately perturbs Wnt signaling, differentiation, and migration. Genes Dev 2004;18:1385–90. [PubMed: 15198980]
24. Luo S, Mao C, Lee B, Lee AS. GRP78/BiP is required for cell proliferation and protecting the inner cell mass from apoptosis during early mouse embryonic development. Mol Cell Biol 2006;26:5688–97. [PubMed: 16847323]
25. Moser AR, Luongo C, Gould KA, McNeley MK, Shoemaker AR, Dove WF. ApcMin: a mouse model for intestinal and mammary tumorigenesis. Eur J Cancer 1995;31a:1061–4. [PubMed: 7576992]
26. Heijmans J, Muncan V, Jacobs RJ, de Jonge-Muller ESM, Graven L, Biemond I, et al. Intestinal tumorigenesis is not affected by progesterone signaling in rodent models. PLoS One 2011;6:e22620.
27. Wang F, Flanagan J, Su N, Wang LC, Bui S, Nielson A, et al. RNAscope: a novel in situ RNA analysis platform for formalin-fixed, paraffin-embedded tissues. J Mol Diagn 2012;14:22–9. [PubMed: 22166544]
28. Sato T, Stange DE, Ferrante M, Vries RG, Van Es JH, Van den Brink S, et al. Long-term expansion of epithelial organoids from human colon, adenoma, adenocarcinoma, and Barrett's epithelium. Gastroenterology 2011; 141:1762–72. [PubMed: 21889923]
29. Sato T, Vries RG, Snippert HJ, van de Wetering M, Barker N, Stange DE, et al. Single Lgr5 stem cells build crypt-villus structures in vitro without a mesenchymal niche. Nature 2009;459:262–5. [PubMed: 19329995]
30. Greten FR, Eckmann L, Greten TF, Park JM, Li Z-W, Egan LJ, et al. IKKbeta links inflammation and tumorigenesis incitat a mouse model of colitis-associated cancer. Cell 2004;118:285–96. [PubMed: 15294155]
31. Zheng L, Kelly CJ, Colgan SP. Physiologic hypoxia and oxygen homeostasis in the healthy intestine. A review in the theme: cellular responses to hypoxia. Am J Physiol Cell Physiol 2015;309:C350–60. [PubMed: 26179603]
32. Montgomery RK, Carlone DL, Richmond CA, Farilla L, Kranendonk MEG, Henderson DE, et al. Mouse telomerase reverse transcriptase (mTert) expression marks slowly cycling intestinal stem cells. Proc Natl Acad Sci U S A 2011;108:179–84. [PubMed: 21173232]
33. Sangiorgi E, Capecchi MR. Bmi1 is expressed in vivo in intestinal stem cells. Nat Genet 2008;40:915–20. [PubMed: 18536716]
34. Tian H, Biehs B, Warming S, Leong KG, Rangell L, Klein OD, et al. A reserve stem cell population in small intestine renders Lgr5-positive cells dispensable. Nature 2011;478:255–9. [PubMed: 21927002]
35. Vogelstein B, Fearon ER, Hamilton SR, Kern SE, Preisinger AC, Leppert M, et al. Genetic alterations during colorectal-tumor development. N Engl J Med 1988;319:525–32. [PubMed: 2841597]
36. Fearon ER. Molecular genetics of colorectal cancer. Annu Rev Pathol 2011;6:479–507. [PubMed: 21090969]
37. Faller WJ, Jackson TJ, Knight JR, Ridgway RA, Jamieson T, Karim SA, et al. mTORC1-mediated translational elongation limits intestinal tumour initiation and growth. Nature 2015;517:497–500. [PubMed: 25383520]
38. Sato T, van Es JH, Snippert HJ, Stange DE, Vries RG, van den Born M, et al. Paneth cells constitute the niche for Lgr5 stem cells in intestinal crypts. Nature 2011;469:415–8. [PubMed: 21113151]
39. van de Wetering M, Sancho E, Verweij C, de Lau W, Oving I, Hurlstone A, et al. The beta-catenin/TCF-4 complex imposes a crypt progenitor phenotype on colorectal cancer cells. Cell 2002;111:241–50. [PubMed: 12408868]
40. Ruggero D. The role of Myc-induced protein synthesis in cancer. Cancer Res 2009;69:8839–43. [PubMed: 19934336]
41. Rosekrans SL, Heijmans J, Buller NV, Westerlund J, Lee AS, Muncan V, et al. ER stress induces epithelial differentiation in the mouse oesophagus. Gut 2015;64:195–202. [PubMed: 24789843]

42. van Galen P, Kreso A, Mbong N, Kent DG, Fitzmaurice T, Chambers JE, et al. The unfolded protein response governs integrity of the haematopoietic stem-cell pool during stress. Nature 2014;510:268–72. [PubMed: 24776803]

43. Metcalfe C, Kljavin NM, Ybarra R, de Sauvage FJ. Lgr5þ stem cells are indispensable for radiation-induced intestinal regeneration. Cell Stem Cell 2014;14:149–59. [PubMed: 24332836]

44. Lee AS, Brandhorst S, Rangel DF, Navarrete G, Cohen P, Longo VD, et al. Effects of prolonged GRP78 haploinsufficiency on organ homeostasis, behavior, cancer and chemotoxic resistance in aged mice. Sci Rep 2017;7:40919. [PubMed: 28145503]

45. Dong D, Stapleton C, Luo B, Xiong S, Ye W, Zhang Y, et al. A critical role for GRP78/BiP in the tumor microenvironment for neovascularization during tumor growth and metastasis. Cancer Res 2011;71:2848–57. [PubMed: 21467168]

46. Wey S, Luo B, Tseng CC, Ni M, Zhou H, Fu Y, et al. Inducible knockout of GRP78/BiP in the hematopoietic system suppresses Pten-null leukemogenesis and AKT oncogenic signaling. Blood 2012;119:817–25. [PubMed: 21937694]

47. Shen J, Ha DP, Zhu G, Rangel DF, Kobielak A, Gill PS, et al. GRP78 haploinsufficiency suppresses acinar-to-ductal metaplasia, signaling, and mutant Kras-driven pancreatic tumorigenesis in mice. Proc Natl Acad Sci U S A 2017;114:E4020–9. [PubMed: 28461470]

Significance:

Heterozygous disruption of chaperone protein Grp78 reduces tissue regeneration and expansive growth and protects from tumor formation without affecting intestinal homeostasis.

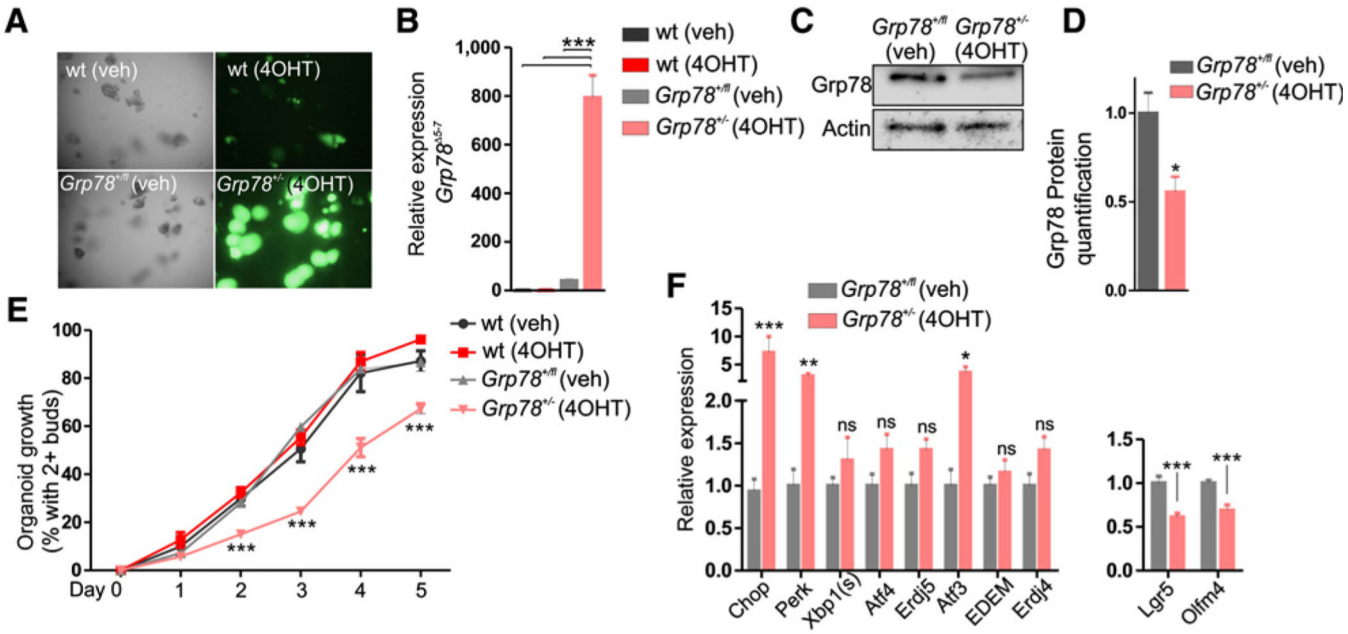

Figure 1.

Grp78 heterozygous organoids exhibit loss of stem cell markers, increase in UPR markers, and impaired growth. **A,** Brightfield and fluorescent images of wild-type and $Grp78^{+/-}$ organoids at day 4 after passaging. **B,** qRT-PCR analysis of floxed $Grp78^{\Delta 5-7}$ *mRNA* in organoids depicted in **A. C,** Western blot analysis for Grp78 protein in nonrecombined and recombined organoids. Actin was used as equal loading control. **D,** Quantification of Western blot analysis in **C,** relative to control. **E,** Organoid growth assessed by the percentage of organoids with two or more buds at indicated times after passaging. **F,** qRT-PCR analysis for UPR components and CBC markers. wt, wild type; veh, vehicle. ns, not significant; **, $P < 0.01$; ***, $P < 0.001$. Original magnification, ×400.

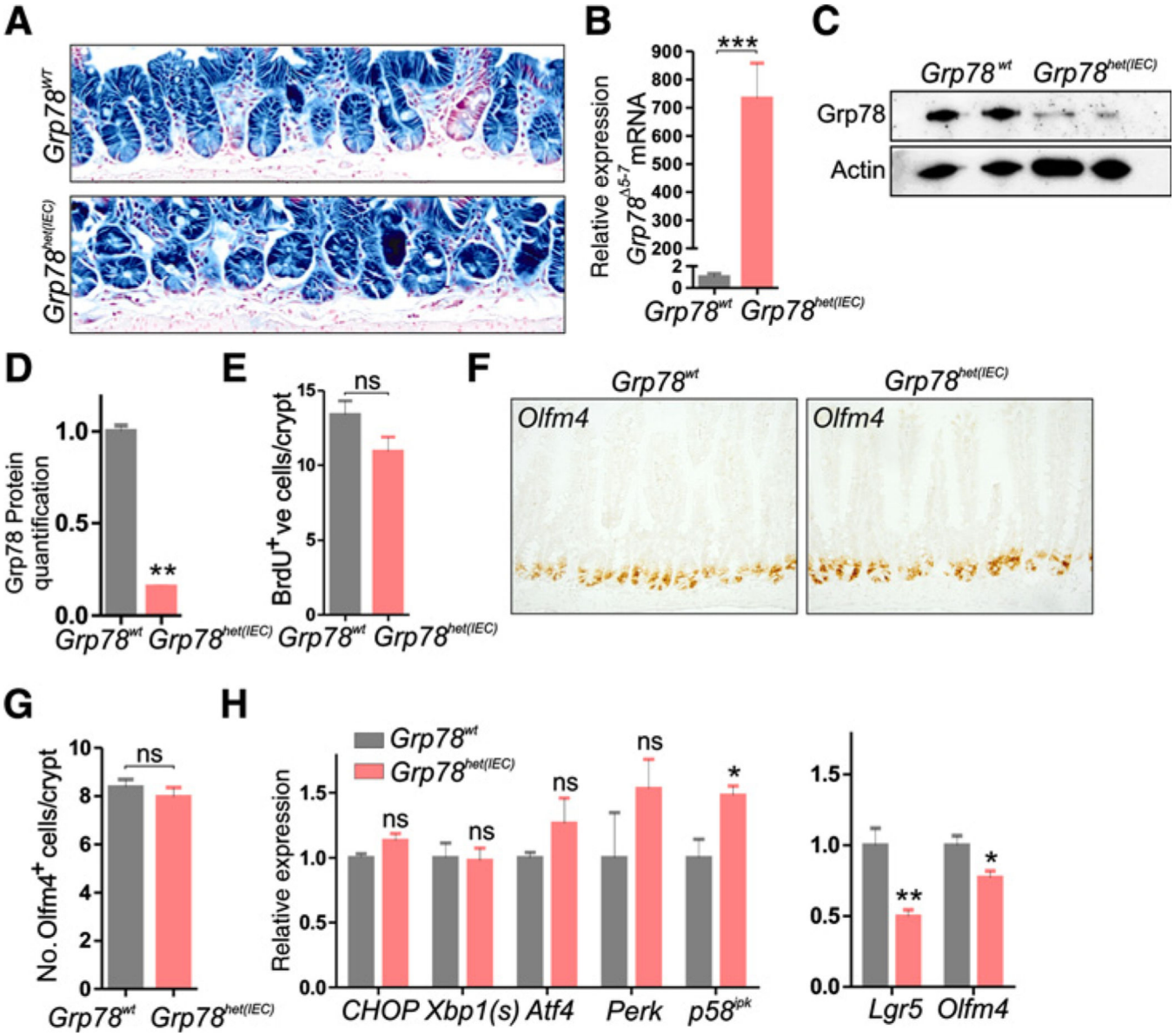

Figure 2.

Grp78 heterozygous mice show unaltered proliferation and stem cell numbers in the intestine. **A,** LacZ staining on intestines of mice showing recombination one month after induction of *Cre*-mediated recombination with tamoxifen. **B,** qRT-PCR analysis offloxed *Grp78*$^{\Delta 5-7}$ *mRNA*. **C,** Western blot analysis for Grp78 protein in nonrecombined and recombined small intestine. Actin was used as equal loading control. **D,** Quantification of Western blot analysis in **C,** relative to control. **E,** Quantification of BrdU-positive cells. **F,** ISH for stem cell marker *Olfm4*. **G,** Quantification of *Olfm4*$^{+ve}$ cells. **H,** qRT-PCR analysis of a panel of UPR components and CBC-stem cell markers *Lgr5* and *Olfm4*. ns, not significant; *, $P < 0.05$; **, $P < 0.01$; ***, $P < 0.001$. Original magnifications, ×200 and ×400.

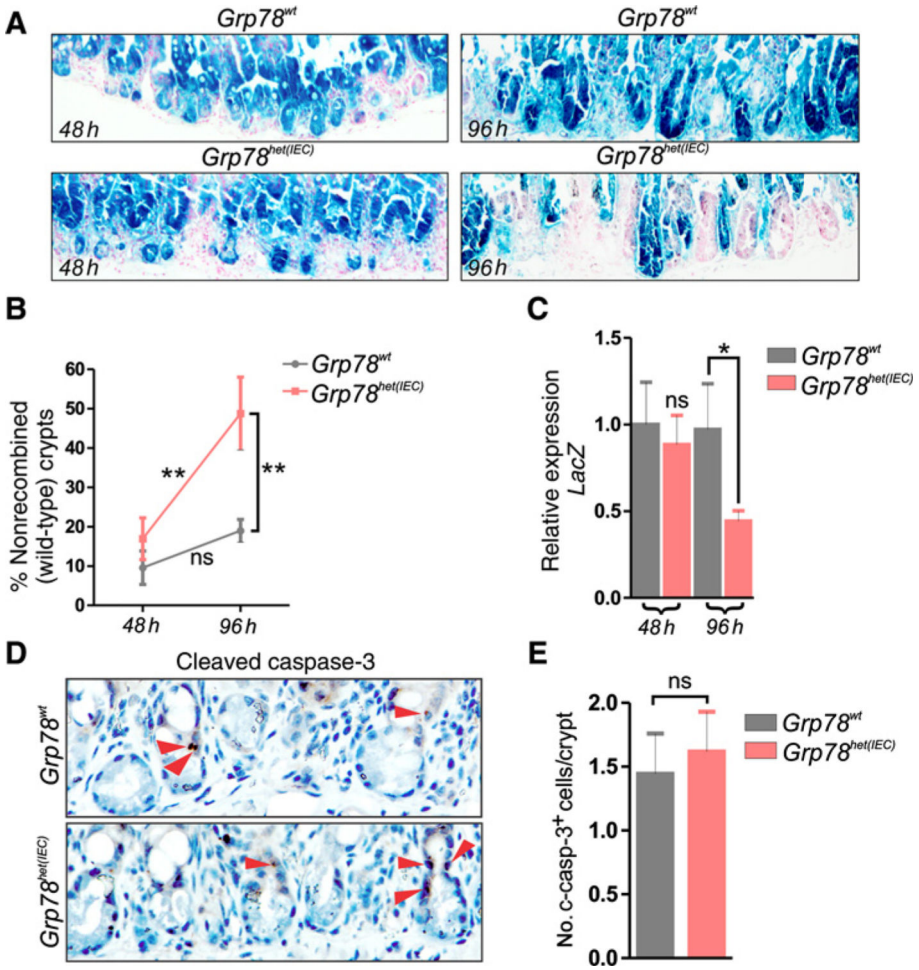

Figure 3.

Regeneration of *Grp78* heterozygous intestinal epithelium after γ-irradiation is favored from nonrecombined stem cells, showing loss of self-renewal capacity in heterozygous intestines. **A,** LacZ staining on small intestines of mice showing recombination 48 hours and 96 hours after irradiation. **B,** Percentage of crypts that are nonrecombined in wild-type control animals and *Grp78*$^{het(IEC)}$ animals, 48 hours and 96 hours after irradiation. **C,** qRT-PCR for expression of LacZ *mRNA*. **D,** IHC for cleaved-caspase-3 at 48 hours postirradiation. Red arrows, positive cells. **E,** Quantification of cleaved-caspase-3–positive cells. ns, not significant; *, $P < 0.05$; **, $P < 0.01$. Original magnification, ×400.

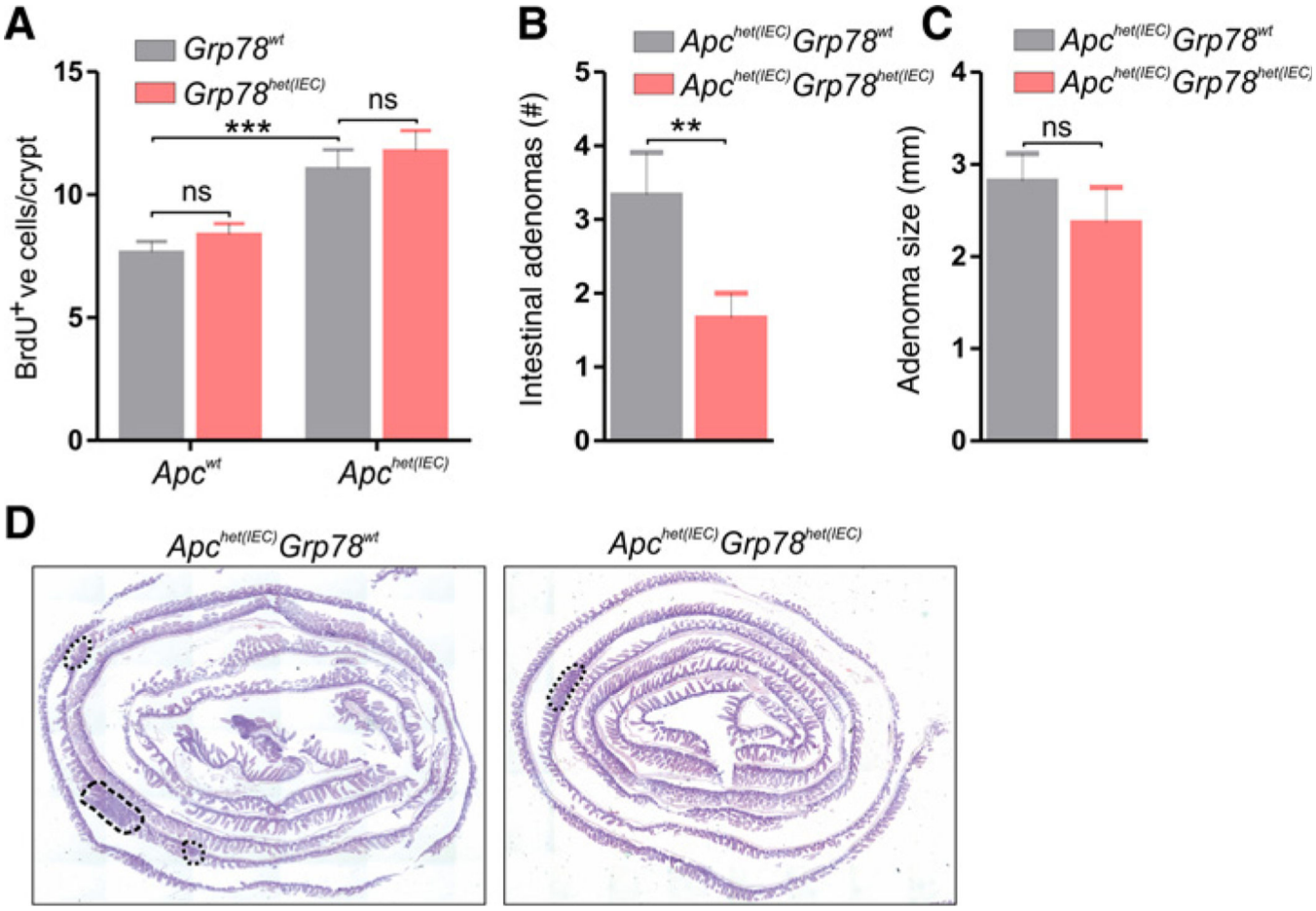

Figure 4.

Reduced adenoma formation in *Grp78* heterozygous mice. **A,** Quantification of IHC for BrdU on mice with indicated genotypes. **B,** Number of adenomas in small and large intestines of mice with indicated genotypes. All animals were sacrificed at the age of 20 weeks, 16 weeks after recombination with tamoxifen. **C,** Average adenoma size in millimeters (mm) of all adenomas. **D,** Representative images (hematoxylin and eosin staining) showing adenomas in the entire small intestine of indicated genotypes. ns, not significant; **, $P < 0.01$.

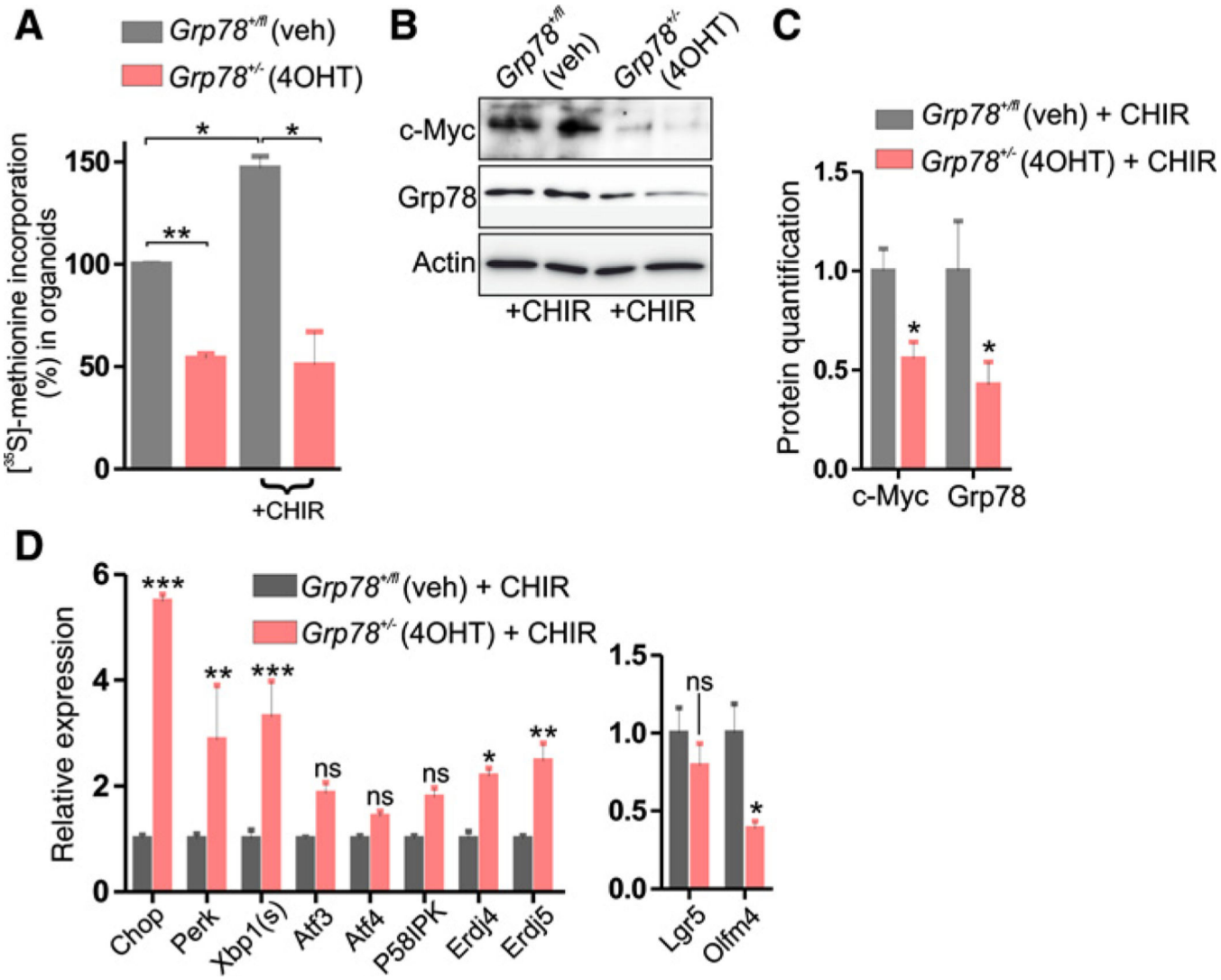

Figure 5.

Reduced protein synthesis in *Grp78* heterozygous organoids and increased ER stress in presence of Wnt pathway activating compound CHIR-99021. **A,** 35S-methionine labeling assay of organoids of indicated genotypes, grown in normal culture medium or with the addition of 5 μmol/L CHIR-99021. **B,** Western blot analysis for c-Myc and Grp78 protein in organoids, with the addition of 5 μmol/L CHIR-99021. **C,** Quantification of Western blot analysis in **B,** relative to control. veh, vehicle. ns, not significant; *, $P < 0.05$; **, $P < 0.01$; ***, $P < 0.001$.